

## Note

To Erika Neeft For information  
 From Tano Kivits & Jasper Griffioen  
 Subject Results of groundwater isotope measurements for  
 the geochemical characterization of the Watervliet  
 Member  
 Attachment(s)

[www.tno.nl](http://www.tno.nl)  
 tano.kivits@tno.nl  
 +31621275559

Date  
 19 February 2026

# 1. Introduction

This note describes the results of the isotope measurements of the groundwater samples that were collected for the geochemical characterization of the Watervliet Member in September 2024. The original groundwater results are discussed in the report “*Geochemical characterisation of the Watervliet Member and groundwater in Paleogene and other sandy units of Zeeland*”<sup>1</sup>. Due to longer analysis time of several isotope measurements and technical difficulties in the laboratory, the isotope measurements from the groundwater samples were not available in time to be included in the original report. This note discusses these results and serves as an addition to the original report.

The 15 groundwater samples, collected in September 2024, were sampled for the analysis of the water isotopes ( $\delta^{18}\text{O}$  and  $\delta^2\text{H}$ ), carbon isotopes of dissolved inorganic carbon ( $^{14}\text{C}$  and  $\delta^{13}\text{C}$ ), and the isotope ( $\delta^{37}\text{Cl}$ ) of dissolved chloride. The results for these individual isotopes are discussed below, followed by an integrated interpretation.

The work described in the afore mentioned main report, as well as the work in this note and another note on clay mineralogy and elemental composition of minerals, received funding from the Ministry of Infrastructure and Water Management.

# 2. Isotope results

## 2.1. Water isotopes

The water isotopes ( $\delta^{18}\text{O}$  and  $\delta^2\text{H}$ ) were analysed by the Institut de Physique du Globe de Paris (IPGP), part of the Université Paris Cité. The isotopes of water, and mainly the oxygen isotope  $^{18}\text{O}$ , are used in hydrology to understand processes of infiltration and evaporation and can be used to give an indication of the origin of the groundwater.

Oxygen-18 is heavier than the regular isotope of oxygen ( $^{16}\text{O}$ ) because of the two extra neutrons in its atomic nucleus. During evaporation of water the molecules existing of  $^{16}\text{O}$  will therefore evaporate more easily than those existing of  $^{18}\text{O}$ . The reverse is the case during rainfall: the heavier  $^{18}\text{O}$  will rain out more easily than  $^{16}\text{O}$ . Oceanic water is therefore enriched in  $^{18}\text{O}$ , and rainwater close to coastal areas will have higher  $^{18}\text{O}$  content than rainwater further inland.

The oxygen isotope of water is noted as the delta between  $^{18}\text{O}$  and  $^{16}\text{O}$  (written as  $\delta^{18}\text{O}$ ) and is given in ‰VSMOW (Vienna Standard Mean Ocean Water). Seawater has, by definition, an average  $\delta^{18}\text{O}$  content

<sup>1</sup> Hoving, A., Kivits, T., Griffioen, J. (2024). *Geochemical characterisation of the Watervliet Member and groundwater in Paleogene and other sandy units of Zeeland*. TNO 2024 R12632.

of 0 ‰VSMOW. The average isotopic composition for precipitation in the Netherlands for  $\delta^{18}\text{O}$  and  $\delta^2\text{H}$  is  $7.40 \pm 2.05$  ‰VSMOW and  $-49.13 \pm 15.17$  ‰VSMOW, respectively (IAEA/WMO, 2025).

Low values of  $\delta^{18}\text{O}$  indicate colder temperatures during precipitation (or larger distance from the coast at continental scale). This can be used to distinguish infiltrating water from the River Rhine which is fed from melting snow and ice from the Alps and groundwater from rainwater that fell in the Netherlands. Lower values of  $\delta^{18}\text{O}$  can also be an indication of paleowater which has infiltrated during glacial periods in the Pleistocene. Heightened values for  $\delta^{18}\text{O}$  in groundwater, compared to the values for current rainwater, can be an indication for a mixture with infiltrating seawater, or a system where large-scale evaporation before infiltration has taken place, such as in marsh- or peatlands.

[Figure 2.1](#) shows the depth plot of the  $\delta^{18}\text{O}$  values in the groundwater samples. The values are in general above those found in local rainwater, indicating either a mixture with seawater or a situation where evaporation has taken place before infiltration. Infiltration during a cold period such as an ice age seems unlikely for these samples. There are several shallow samples which show high  $\delta^{18}\text{O}$  values (above  $-4.0\text{‰VSMOW}$ ). These are clearly linked with seawater intrusion, the depth pattern is similar to that of the chloride concentrations in the groundwater samples (see right plot of [Figure 2.1](#)).

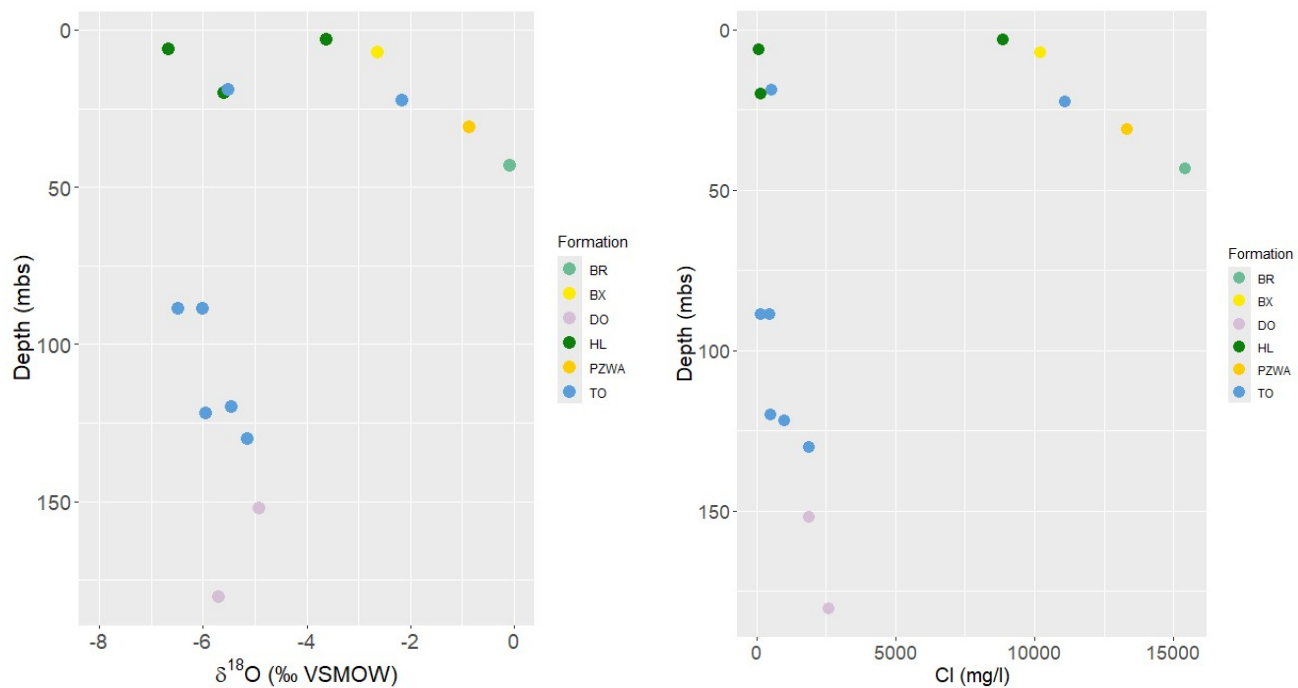


[Figure 2.1](#): Left: Depth plot of  $\delta^{18}\text{O}$  (in ‰VSMOW) of the groundwater samples. Right: depth plot of Cl (in mg/l) of the groundwater samples. The colours indicate the different formations that the sampled groundwater wells belong to.

The relation between  $\delta^{18}\text{O}$  and the chloride concentrations is shown in [Figure 2.2](#), with the black line indicating the mixing line between local rainwater (bottom left) and seawater (top right). Generally, the values are closely related to each other and follow the mixing line between rainwater and seawater quite well. All values are to the right of the mixing line, however, indicating that the  $\delta^{18}\text{O}$  is higher than can be explained by solely a mixture of recent rainwater with seawater. This likely means that the infiltrating water has undergone some evaporation before infiltrating into the groundwater. This could be the case for older water infiltrated during warmer periods in the Holocene where peatland covered a large part of Zee-land.

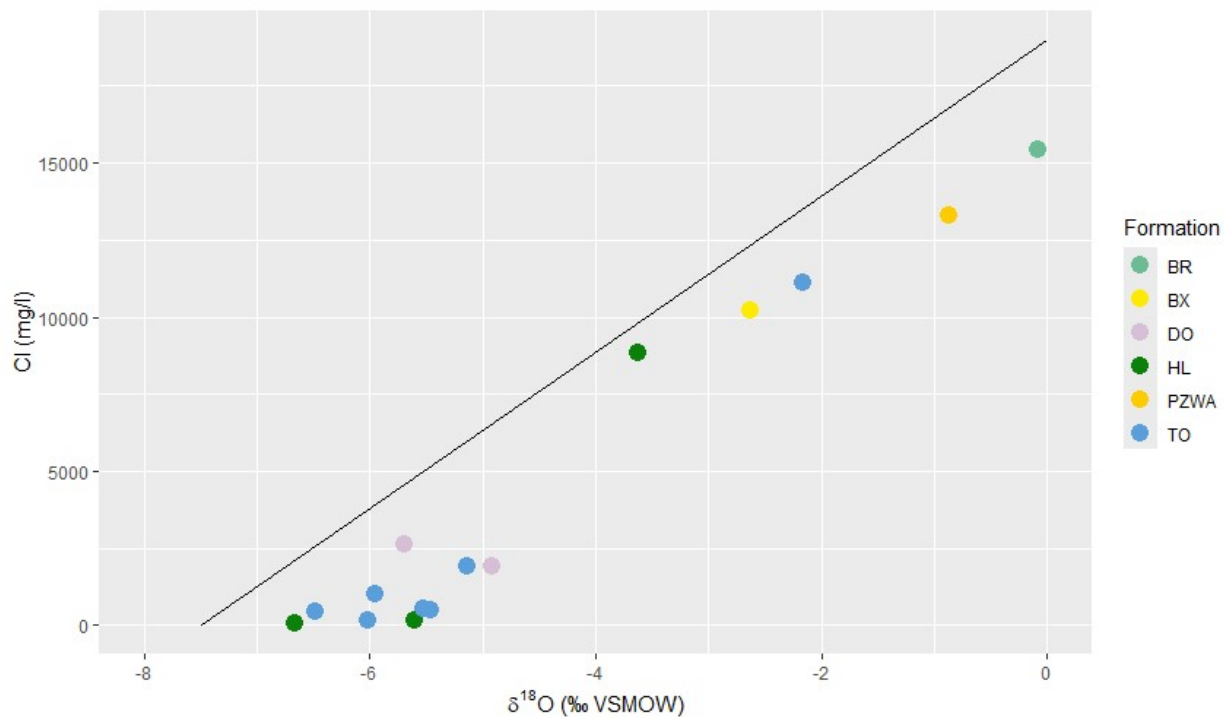


**Figure 2.2:** Plot of  $\delta^{18}\text{O}$  (in ‰ VSMOW) versus the chloride concentrations (in mg/l). The black line indicates the mixing line between rainwater and seawater. The colours indicate the different formations that the sampled groundwater wells belong to.

Next to  $\delta^{18}\text{O}$ , the isotope ratio of hydrogen ( $\delta^2\text{H}$ ) was also measured. The same processes that cause fractionation of the oxygen isotope also occur for the hydrogen isotope, which is why there is a clear relation between these two. This relation is known as the Meteoric Water Line (see [Figure 2.4](#)). The Meteoric Water Line varies per location. Globally, the relation between  $\delta^2\text{H}$  and  $\delta^{18}\text{O}$  is as follows:

$$\delta^2\text{H} = 8 \delta^{18}\text{O} + 10\text{‰}$$

This relation is known as the Global Meteoric Water Line (or GMWL). Based on measurements of the water isotopes in the Global Network of Isotopes in Precipitation (GNIP), Local Meteoric Water Lines (LMWL) can be drawn up. For the samples taken in this project, the closest GNIP station is Braakman (in Zeeuws-Vlaanderen). For this location, there are monthly measurements available between 1994 and 2009, shown in [Figure 2.3](#). The large spread in the data can be explained by seasonal differences in the isotopic composition of the rainwater: during colder months the  $\delta^2\text{H}$  and  $\delta^{18}\text{O}$  of rainwater are lighter than during warmer months. In (deeper) groundwater systems, these seasonal fluctuations are averaged out to the values reported above. By using linear regression through the measurements, it is possible to create a LMWL which is more suitable for the locations of the groundwater wells sampled. The LWML is determined as follows:

$$\delta^2\text{H} = 7.05 \delta^{18}\text{O} + 2.54\text{‰}$$

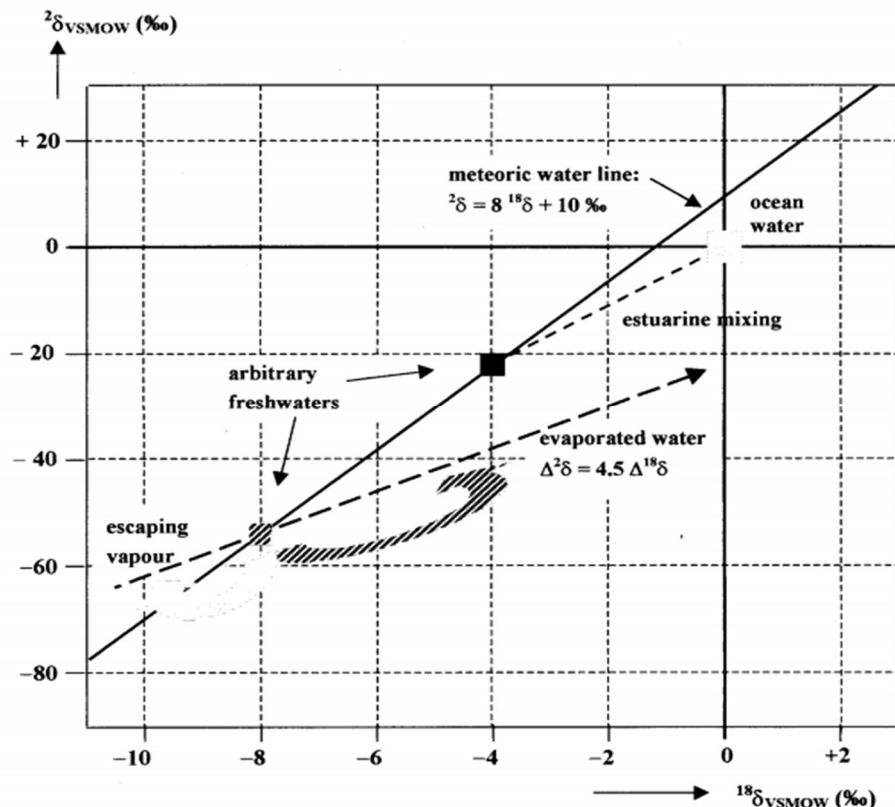


Figure 2.4: Relation between  $\delta^{18}\text{O}$  (x-axis) and  $\delta^2\text{H}$  (y-axis, both in VSMOW), also known as the Meteoric Water Line. The plot includes different effects such as the mixing line between fresh water and ocean water (estuarine mixing) and water under the influence of evaporation. From Mook, 2000.

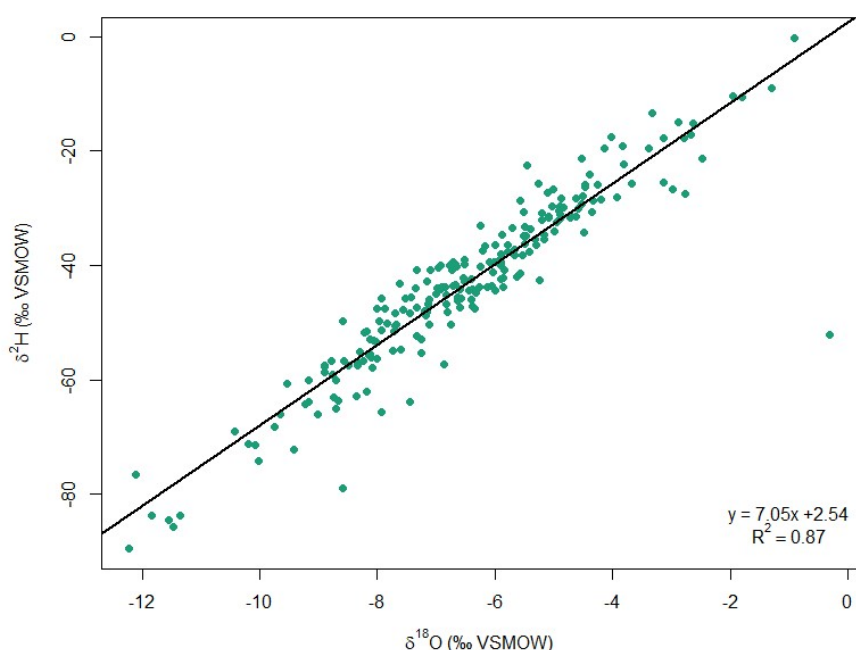


Figure 2.3: Monthly measurements of  $\delta^{18}\text{O}$  and  $\delta^2\text{H}$  (both in ‰ VSMOW) in rainwater for the GNIP location Braakman between the years 1994 and 2009. The Local Meteoric Water Line of this location is determined using linear regression (black line), resulting in a line with formula  $y = 7.05x + 2.54$  and a  $R^2$  of 0.87.

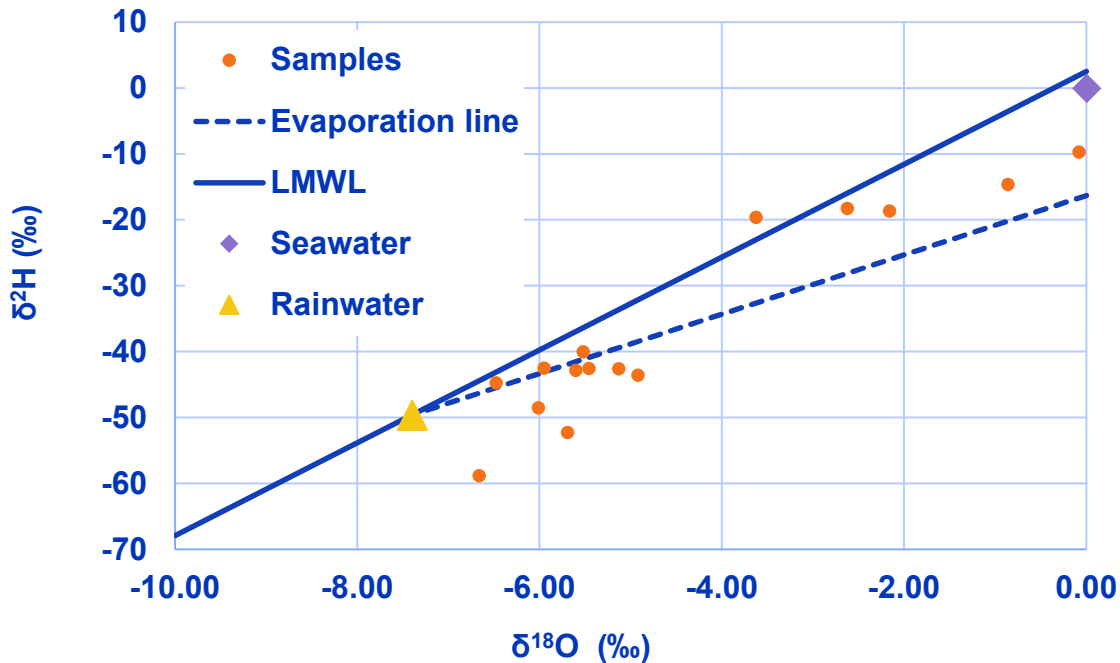


Figure 2.5: Plot of  $\delta^{18}\text{O}$  and  $\delta^2\text{H}$  (both in ‰ VSMOW). The orange point show the measurements of the groundwater wells. The line indicates the LMWL following the measurements from precipitation of GNIP station Braakman (see Figure 2.3), with the dashed line indicating the evaporation line from the rainwater

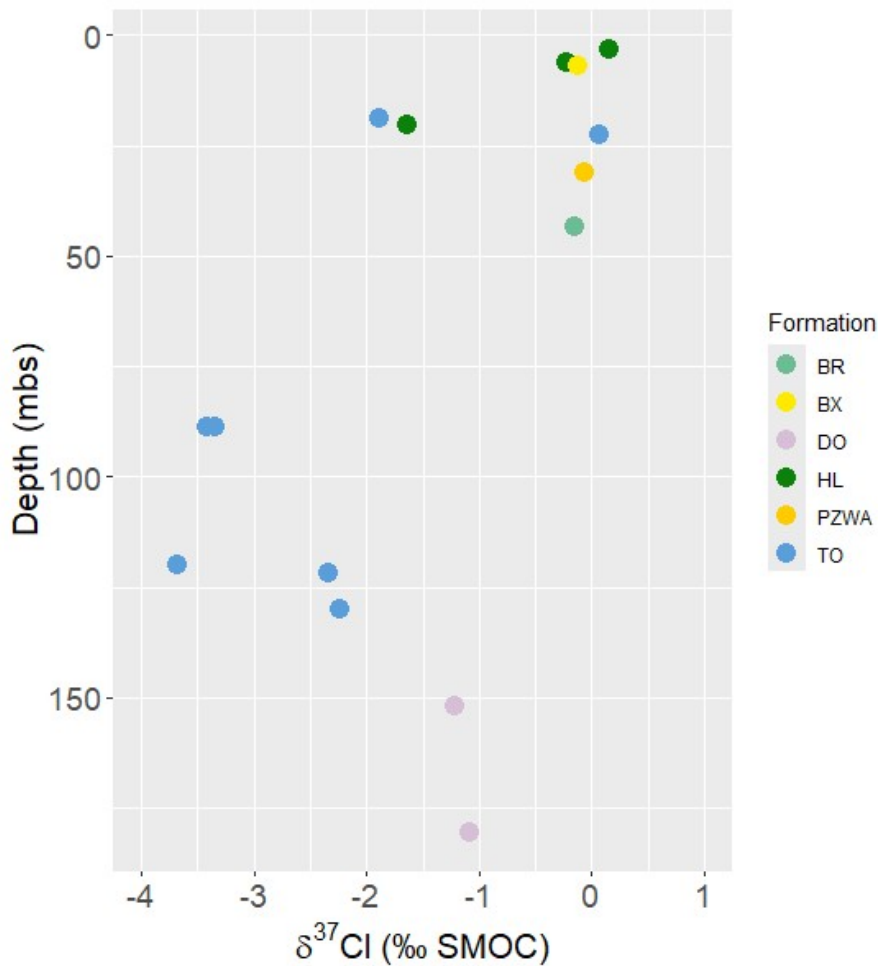
Changes from the meteoric water line can be used to give an indication of the origin of the groundwater samples, and processes such as evaporation and seawater intrusion. The results for the groundwater samples are shown in Figure 2.5. In this plot, the samples are shown together with the LMWL, the evaporation line with relation  $\delta^2\text{H} = 4.5 \delta^{18}\text{O}$  (Figure 2.4), and the average rainwater and seawater positions. Most samples plot below the LMWL, indicating a general enrichment of  $\delta^{18}\text{O}$  in relation to  $\delta^2\text{H}$ . This can be explained by evaporative processes before infiltration, where  $\delta^2\text{H}$  undergoes stronger kinetic fractionation than  $\delta^{18}\text{O}$ . This is in line with the relation between  $\delta^{18}\text{O}$  and the chloride concentrations (Figure 2.2). This also goes for the samples which plot closer to the seawater endpoint and with high chloride concentrations: these plot mostly below the LMWL, so evaporation in an estuarine environment seems likely. The only sample above the LMWL is from a very shallow well (WV10 with a filter depth of 2.5-3.5 m below surface). This is most likely groundwater heavily influenced by very recent rainwater, the value is within the bandwidth of the rainwater values of Figure 2.3. The strongest deviation from the LMWL is the sample with the lowest  $\delta^2\text{H}$ : WV01 at 6 m below surface with a  $\delta^2\text{H}$  of -59‰ and  $\delta^{18}\text{O}$  of -6.7‰. The strong evaporative effect from this sample could possibly be explained by the effects of irrigation: the well is next to agricultural fields and high evaporation during the spraying of water might cause the lower  $\delta^2\text{H}$  relative to the  $\delta^{18}\text{O}$  value.

## 2.2. $\delta^{37}\text{Cl}$

Next to the water isotopes,  $\delta^{37}\text{Cl}$  from dissolved chloride was also measured by IPGP. Chloride is usually a conservative solute in groundwater, which means that the natural variations between the stable isotopes are small. The relation between  $^{37}\text{Cl}$  and  $^{35}\text{Cl}$ , noted as  $\delta^{37}\text{Cl}$  in ‰ SMOC (Standard Mean Ocean Chlorine) can therefore be used to indicate processes which cause limited fractionation such as diffusion, ion-exchange and salt precipitation. Diffusion may be noted when there are gradients between lower and higher chloride concentrations, where the lighter  $^{35}\text{Cl}$  has a higher diffusion coefficient than the

heavier  $^{37}\text{Cl}$  due to its lower atomic mass. Therefore, if the chloride concentration in groundwater is (partly) caused by diffusion, for example from out of clay layers, the  $\delta^{37}\text{Cl}$  content will be lower. These diffusion processes tend to be slow, so a lowered  $\delta^{37}\text{Cl}$  indicates that there has been limited to no groundwater flow and the water can be considered to be stagnant.

The results for  $\delta^{37}\text{Cl}$  are shown in the depth plot of Figure 2.6. In this plot, several groups are distinguished. Most of the shallow samples (<50 m below surface) have a  $\delta^{37}\text{Cl}$  of around 0‰, indicating that the chloride in these samples is not caused by diffusion and that the groundwater in these wells likely undergoes some flow. Two shallow samples show lower  $\delta^{37}\text{Cl}$  values: well B54B0093 (Pyramide) in the Tongeren Formation at a depth of 19 meters below surface, and the fourth filter of well B48G0100 (Ovezande) in Holocene formations (Koewacht) at a depth of 20 m below surface. These values are somewhat surprising, the groundwater does not seem to be confined by significant aquitards at this depth.



aquifer or chloride has diffused out of an adjacent clay layer that may contain higher Cl concentrations, i.e., more saline, than the sampled aquifer. The brackish samples of the Dongen Formation have  $\delta^{18}\text{O}$  and  $\delta^2\text{H}$  values that coincide with the fresh samples, which indicates that these Cl concentrations are merely controlled by diffusion and not by mixing between fresh water and seawater as the shallow, saline samples.

## 2.3. $^{14}\text{C}$ and $\delta^{13}\text{C}$

Next to the water and chlorine isotopes, the carbon isotopes of the Dissolved Inorganic Carbon ( $^{14}\text{C}$ -DIC and  $\delta^{13}\text{C}$ -DIC) were also determined. The analysis was performed by the Centre of Isotope Research of the University of Groningen.  $^{14}\text{C}$ arbon is a radioactive isotope of carbon which is used for age dating of carbon-containing materials, and can also be used to date groundwater from dissolved DIC. Because of its relatively long half-life of 5,730 years, it is most suited for dating groundwater with an age range from about 1,000 to 40,000 years old.  $^{14}\text{C}$  values are expressed as a percentage of modern carbon (pmC), where 100 pmC represents the  $^{14}\text{C}$  content of recent material.

Figure 2.7 shows the depth plot of the  $^{14}\text{C}$  values of the groundwater samples. All samples in the upper part of the subsurface have relatively high  $^{14}\text{C}$  values (60-97 pmC), indicating that these likely consist of young water. There is a clear distinction between the samples above the Rupel Formation (Boom Clay) and below: the  $^{14}\text{C}$  values in the deeper Tongeren and Dongen formation are lower (< 10 pmC), indicating that the groundwater at these depths is likely to be much older.

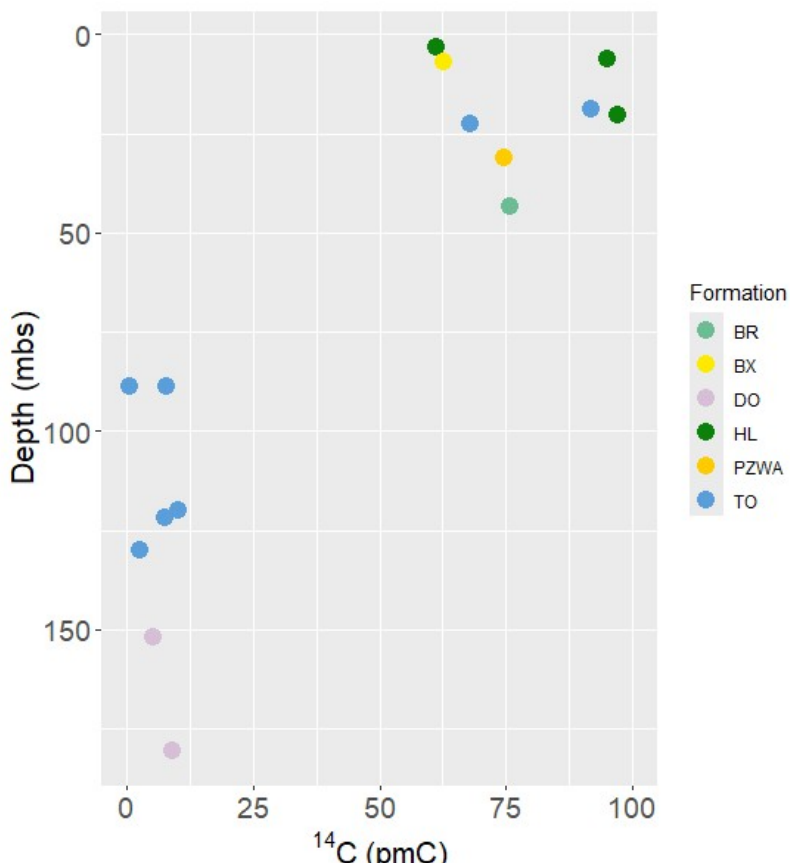


Figure 2.7: Depth plot of  $^{14}\text{C}$ -DIC (percent modern Carbon) in the groundwater samples. The colours indicate the different formations that the sampled groundwater wells belong to.

The  $^{14}\text{C}$  values of the groundwater samples can be used to make an estimate of the groundwater age, known as the  $^{14}\text{C}$ -apparent age. The  $^{14}\text{C}$ -apparent age of groundwater can be calculated by the following formula (Clark & Fritz, 1997):

$$T = -\frac{5730}{\ln 2} \times \ln \left[ \frac{^{14}\text{C}_{\text{sample}}}{^{14}\text{C}_0} \right]$$

with  $T$  being the  $^{14}\text{C}$ -apparent age,  $^{14}\text{C}_{\text{sample}}$  the measured carbon-14 content of the sample and  $^{14}\text{C}_0$  the initial  $^{14}\text{C}$  content of the groundwater sample before radioactive decay. Determining this  $^{14}\text{C}_0$  is the critical step in getting a reliable  $^{14}\text{C}$ -apparent age: because of geochemical processes in the subsurface, such as the dissolution of carbonates, there is mixing of  $^{14}\text{C}$ -dead carbon in the subsurface. Modelling the  $^{14}\text{C}_0$  may be very complicated, depending on the hydrogeological setting, the hydrogeochemical processes that affected the carbonate chemistry along the flow path, and the origin and age of the solid or dissolved inorganic carbon. Several methods exist for correcting for these processes (e.g. Han & Plummer, 2016; Blaser et al., 2010; Broers et al., 2021; Stuyfzand et al., 2025), but in this study we limited ourselves by interpreting the maximum  $^{14}\text{C}$ -age with a  $^{14}\text{C}_0$  of 100%. This is an overestimation of the true age of the groundwater, but still useful in determining differences between samples from different depths.

The maximum  $^{14}\text{C}$ -ages for the groundwater samples are given in [Table 4.1](#). Most shallow samples have maximum  $^{14}\text{C}$  ages of less than 1,000 years, these are most likely very recent and too young to give a reliable  $^{14}\text{C}$  age. Given the shallow depth of most of these samples, the  $^{14}\text{C}$  values are actually lower than expected. Some of these could be explained by the dissolution of  $^{14}\text{C}$ -dead carbonates. However, this doesn't seem very likely for some very shallow samples such as WV01, WV10 and WV11, where two screens are installed in Holocene sediments and all three located only a couple of meters below surface. The low  $^{14}\text{C}$  values are difficult to explain under natural conditions, but it seems unlikely that the groundwater is older than 1,000 years at these depths. Possibly, there is a mixture between infiltrating rainwater, seawater, and irrigation water, which makes it difficult to give an exact age for these samples.

The deeper samples in the Tongeren and Dongen formations are all much older with maximum  $^{14}\text{C}$  ages of 18,000 to 41,000 years old. Blaser et al. (2010) and Walraevens et al. (2020) studied  $^{14}\text{C}$ -ages in the Ledo-Paniselian aquifer system in Belgium, which is equivalent to the Dongen Formation in the Netherlands. There, they found similar groundwater ages, but also a gap between 14,000 and 21,000 year old groundwater indicating a colder period during the late Weichselian with permafrost and inhibited infiltration. Samples with maximum  $^{14}\text{C}$  ages in this age range (WV05, WV07, WV14 and WV15) are thus likely to be younger and infiltrated during the Holocene, which is also likely considering the relatively high  $\delta^{18}\text{O}$  values of groundwater itself. Considering the low  $^{14}\text{C}$  activities found for these samples they are still likely to be thousands of years old. The oldest groundwater sample (WV08 – Hulst) has a very low  $^{14}\text{C}$  activity of only 0.7%, nearing the limits of what can be dated by  $^{14}\text{C}$ . The maximum age of this sample is 41,000 years old, most likely being infiltrated in warmer periods during the Weichselian. The  $\delta^{37}\text{Cl}$  content of this sample is also low, indicating old and stagnant water at this location.

The  $\delta^{13}\text{C}$ -DIC analyses show some striking results. Three groups can be recognised ([Figure 2.8](#)): 1. high values close to 0 that are associated with low  $^{14}\text{C}$  content, 2. intermediate values between -4.5 and -10.5‰ with both young and old groundwater according to  $^{14}\text{C}$  results and 3. low values between -13.5 and -16.5‰ associated with high  $^{14}\text{C}$  contents. The last values can be explained as a mixture of carbon from degradation of organic matter (typically around -25‰) and dissolution of marine Ca-carbonate (typically around 0‰). The first values need a major carbonate source having a high  $\delta^{13}\text{C}$ . In first instance, this suggests DIC from methanogenesis but methane concentrations are low in all samples. Associated anaerobic methane oxidation in association with  $\text{SO}_4$ -reduction is also an unsatisfactory

explanation as this would produce DIC with very negative values. Another explanation may be much dissolution from marine carbonates but the DIC and alkalinity values are not exceptionally high compared to the other samples. Both samples are from the Dongen Formation and  $\delta^{37}\text{Cl}$  is also negative with values of -1.76 and -1.62‰. This indicates stagnant conditions and diffusion control. The carbonate chemistry is thus complex in this buried aquifer. The intermediate values can be explained by enhanced dissolution of marine Ca carbonates which is feasible during freshening where Ca becomes adsorbed and carbonates dissolve to compensate for that. The high DIC and alkalinity are also indicative for this.

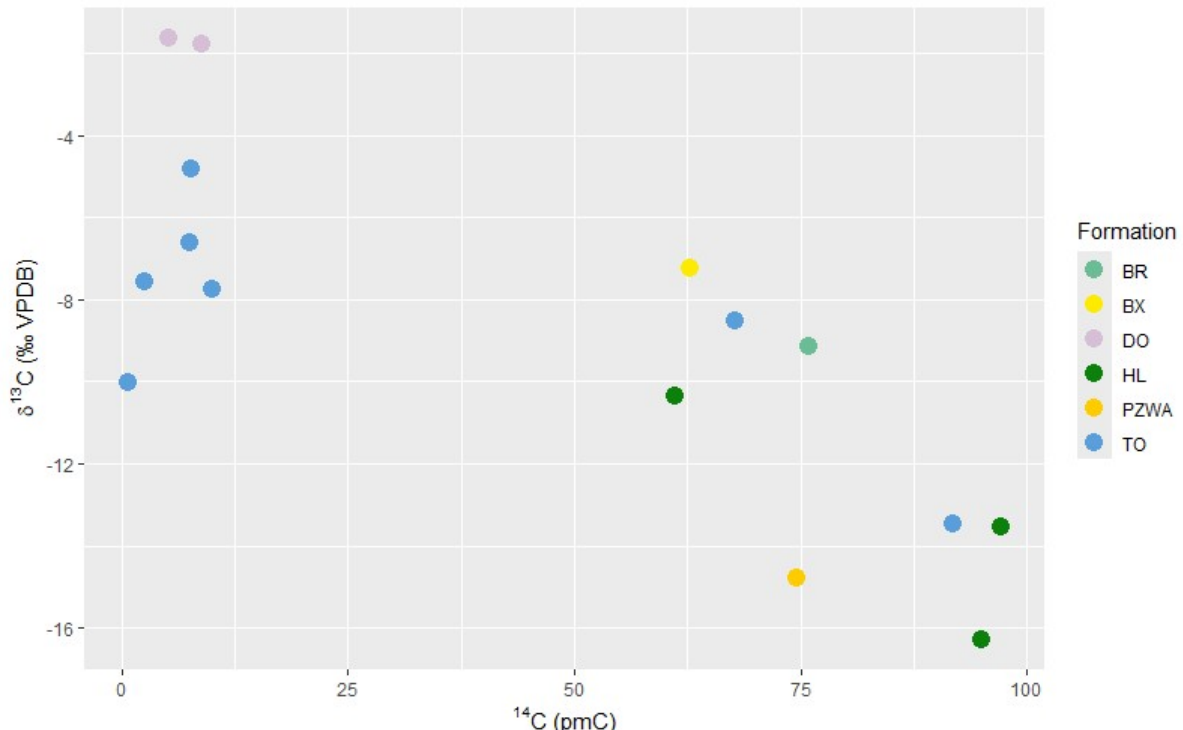


Figure 2.8: Plot of the  $^{14}\text{C}$  and  $\delta^{13}\text{C}$  isotope analyses for dissolved inorganic carbonate in the groundwater samples.

### 3. Synthesis

The measured isotopes show that there is a clear stratification between the shallow and deeper groundwater system. The samples above the Rupel Formation (Boom Clay) are generally much younger with high  $^{14}\text{C}$  activities, indicating recent recharge. In the deeper Tongeren and Dongen formations, the water is much older with low  $^{14}\text{C}$  activities, but still in many cases likely being infiltrated during the Holocene. The  $\delta^{37}\text{Cl}$  results support this zonation: most of the shallow samples have a  $\delta^{37}\text{Cl}$  of around 0‰ indicating active groundwater flow, while the deeper samples, especially those in the Tongeren Formation, have lower  $\delta^{37}\text{Cl}$  values showing diffusion control on groundwater transport and associated stagnant conditions.

The  $\delta^{18}\text{O}$  and  $\delta^2\text{H}$  values in shallow wells are higher than local rainwater and show a clear relation with the chloride concentrations, indicating a mix between rain- and infiltrating seawater. Most samples show

signs of significant evaporation before infiltration, which could be likely in Holocene peatland environments. This is also the case for most of the deeper samples in the Tongeren and Dongen formations, the relative high  $\delta^{18}\text{O}$  values combined with the  $^{14}\text{C}$  activities show that infiltration during the (early) Holocene is the most likely for these samples.

## 4. Isotope analyses

Table 4.1: Results of the measurements of the isotopes of the 15 WV samples.

Sample code	Well	Filter	Location	Sample date	Top of filter (mbs)	Bottom of filter (mbs)	Formation	$\delta^{18}\text{O}$ VSMOW ‰	$\delta^2\text{H}$ VSMOW ‰	$\delta^{37}\text{Cl}$ SMOC ‰	$^{14}\text{C}$ pmC	$\delta^{13}\text{C}$ VPDB ‰	$^{14}\text{C}$ age max
WV01	B48G0100	1	Ovezande	3-9-2024	5.6	6.6	HL	-6.7	-18.0	-0.2	95.0	-16.3	425
WV02	B48G0100	4	Ovezande	3-9-2024	19.66	20.66	HL	-5.6	-9.9	-1.6	97.1	-13.5	243
WV03	B48G0100	5	Ovezande	3-9-2024	30.52	31.52	PZWA	-0.9	-14.6	-0.1	74.6	-14.8	2.428
WV04	B48G0100	6	Ovezande	3-9-2024	42.69	43.69	BR	-0.1	-9.7	-0.2	75.9	-9.2	2.285
WV05	B48G0204	1	Ovezande	4-9-2024	90.92	148.92	TO	-5.5	-42.5	-3.7	10.1	-7.7	18.976
WV06	B48E0224	1	s-Heer Arendskerke	4-9-2024	127.51	132.51	TO	-5.1	-42.6	-2.2	2.6	-7.6	30.311
WV07	B55A0340	1	Hulst	4-9-2024	153.75	207.15	DO	-5.7	-52.2	-1.1	8.9	-1.8	20.025
WV08	B55A0341	1	Hulst	5-9-2024	75.15	102.15	TO	-6.0	-48.5	-3.4	0.7	-10.0	41.274
WV09	B48C0196	1	Groede	10-9-2024	117	187	DO	-4.9	-43.5	-1.2	5.3	-1.6	24.324
WV10	B54E0238	1	Sluiskil	10-9-2024	2.56	3.56	HL	-3.6	1.0	0.2	61.1	-10.4	4069
WV11	B54E0238	2	Sluiskil	10-9-2024	6.53	7.53	BX	-2.6	-18.2	-0.1	62.7	-7.2	3.855
WV12	B54E0238	3	Sluiskil	10-9-2024	21.91	22.91	TO	-2.2	2.2	0.1	67.8	-8.5	3.209
WV13	B54B0093	1	Pyramide	10-9-2024	18.44	19.44	TO	-5.5	-40.0	-1.9	91.8	-13.5	711
WV14	B48H0291	1	Kloosterzande	11-9-2024	93.9	150	TO	-6.0	-10.1	-2.3	7.5	-6.6	21.422
WV15	B54F0093	1	Axel	11-9-2024	76.88	100.38	TO	-6.5	-44.7	-3.3	7.8	-4.8	21.140

## 5. References

Blaser, P.C., Coetsiers, M., Aeschbach-Hertig, W., Kifper, R., Van Camp, M., Loosli, H.H. & Walraevens, K. (2010). A new groundwater radiocarbon correction approach accounting for palaeoclimate conditions during recharge and hydrochemical evolution: The Ledo-Paniselian Aquifer, Belgium. *Applied Geochemistry* 25(3), 437-455. <https://doi.org/10.1016/j.apgeochem.2009.12.011>

Broers, H.P., Süttenfuß, J., Aeschbach, W., Kersting, A., Menkovich, A., de Weert, J. & Castelijns, J. (2021). Paleoclimate signals and groundwater age distributions from 39 public water works in the Netherlands; insights from noble gases and carbon, hydrogen and oxygen isotope tracers. *Water Resources Research*, 57. <https://doi.org/10.1029/2020WR029058>

Clark, I. & Fritz, P. (1997). Environmental Isotopes in Hydrogeology. CRC Press, Boca Raton, New York, 328 pp.

Han, L.F. & Plummer, L., N. (2016). A review of single-sample-based models and other approaches for radiocarbon dating of dissolved inorganic carbon in groundwater. *Earth-Science Reviews*, 152, 119-142 <https://doi.org/10.1016/j.earscirev.2015.11.004>

IAEA/WMO (2025). Global Network of Isotopes in Precipitation. The GNIP Database. Accessible at: <https://nucleus.iaea.org/wiser>

Mook, W.G. (2000). Environmental isotopes in the hydrological cycle. UNESCO.

Walraevens, K., Blaser, P., Aeschbach, W., Van Camp, M. (2020). A palaeoclimate record from the Ledo-Paniselian Aquifer in Belgium – Indications for groundwater recharge and flow in a periglacial environment. *Quaternary International* 547, 147-144. <https://doi.org/10.1016/j.quaint.2019.06.003>